3. Diagnostics

3.1 Optical polarisation

selective extinction

by

elongated dust grains

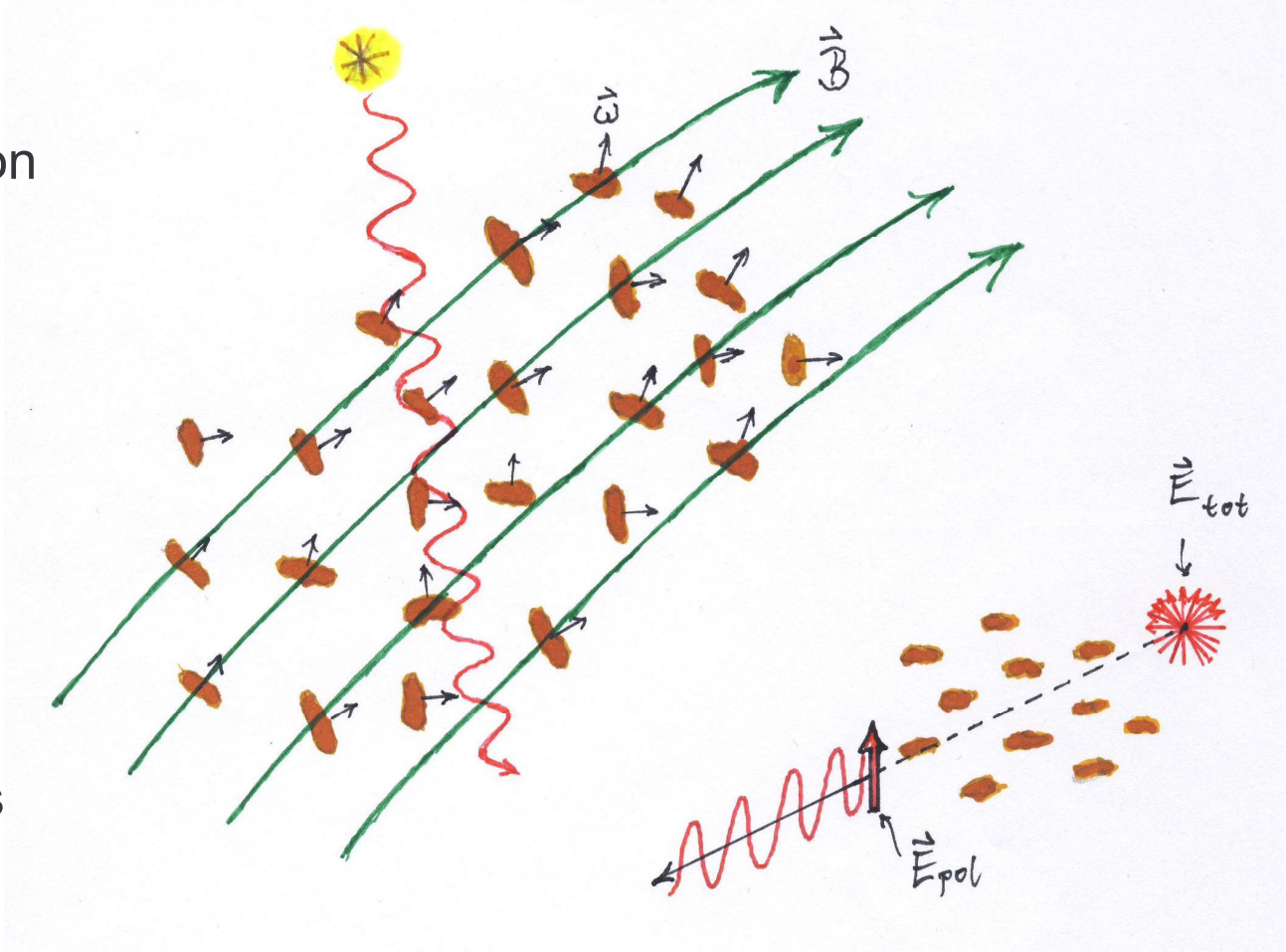

Polarisation of starlight in the Milky Way
(Mathewson & Ford 1970)

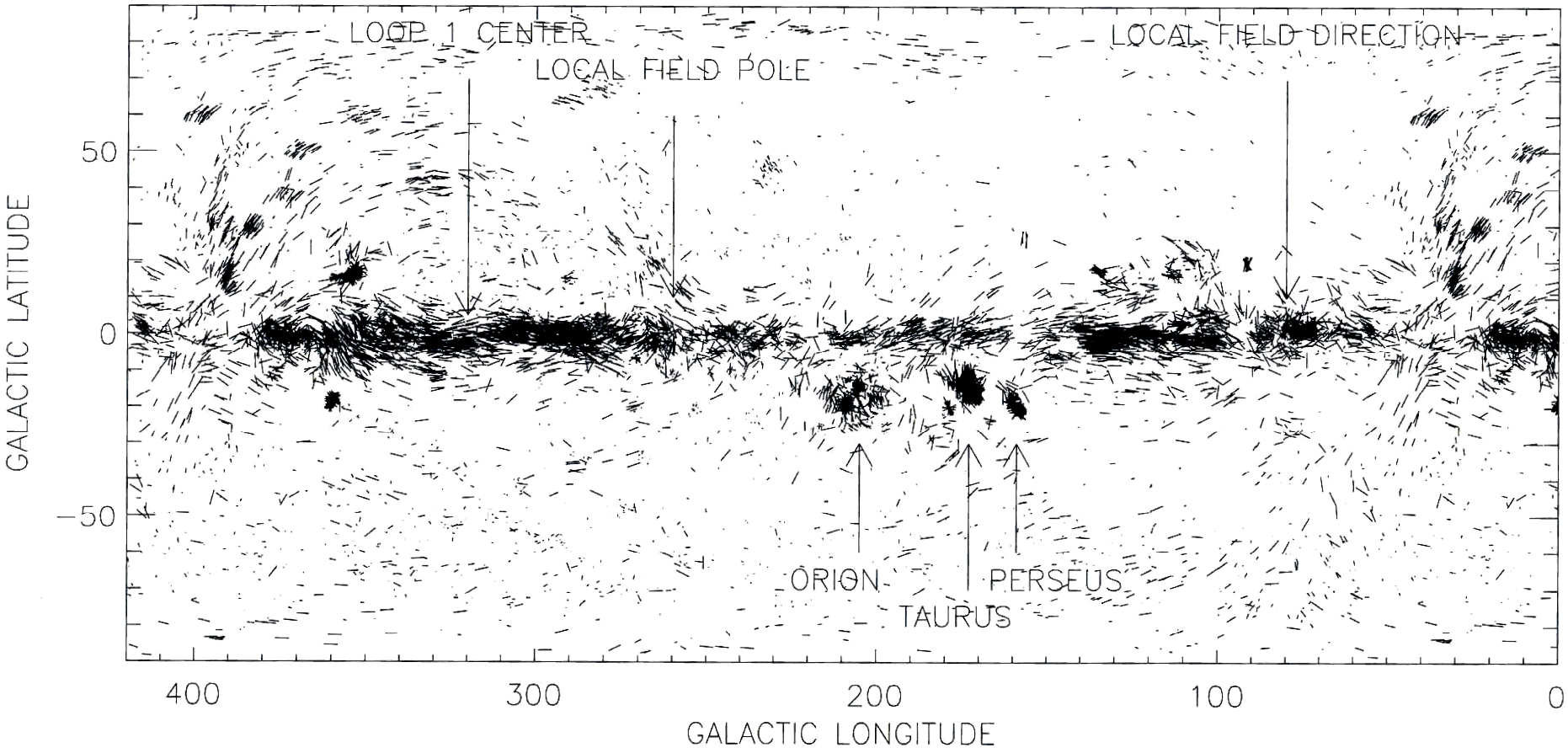

polarisation in M 51:

optical

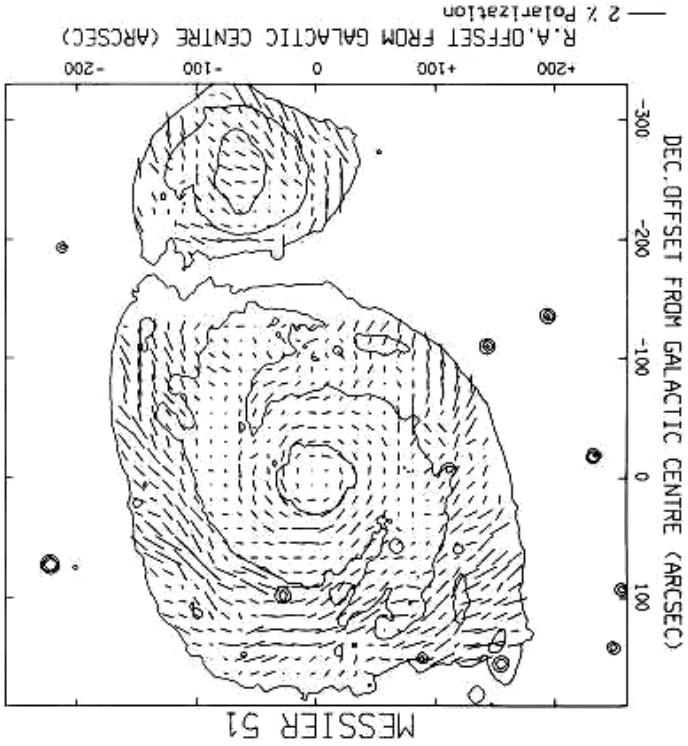

radio

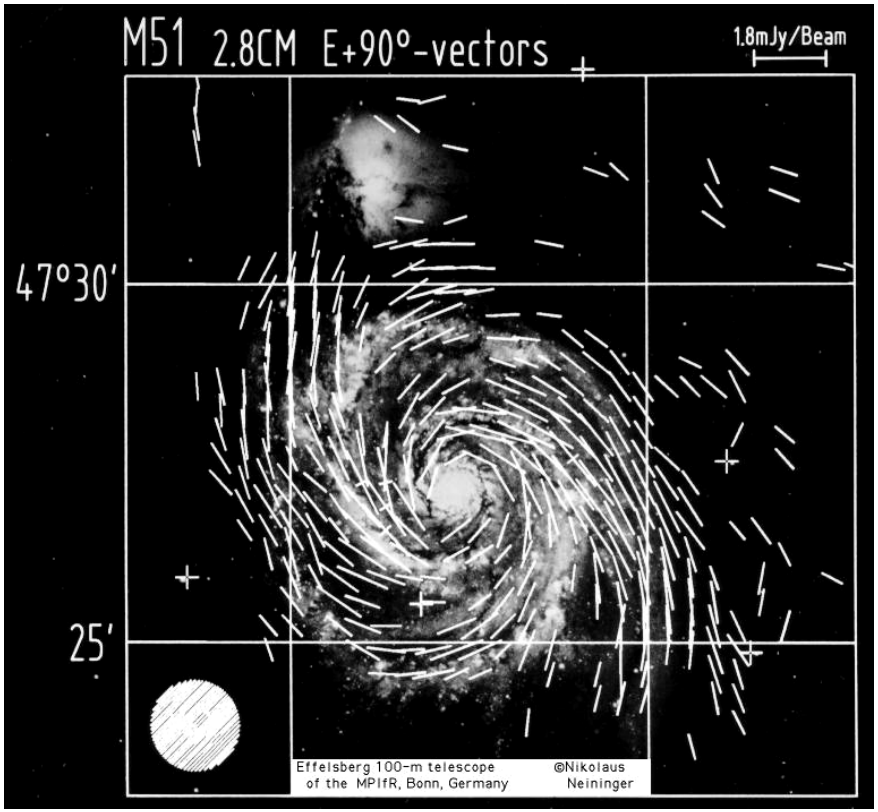

3.2 Synchrotron radiation

minimum energy – equipartition energy

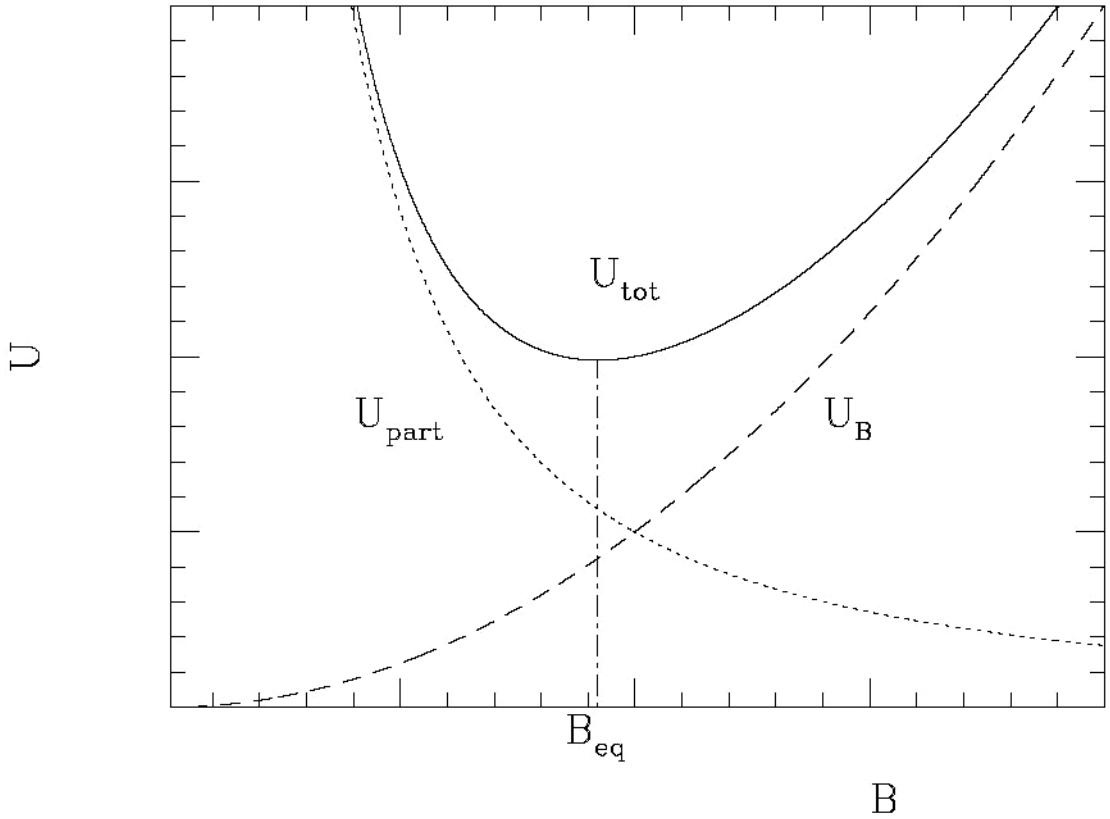

3.2 Faraday rotation

LHC and RHC electro-magnetic waves

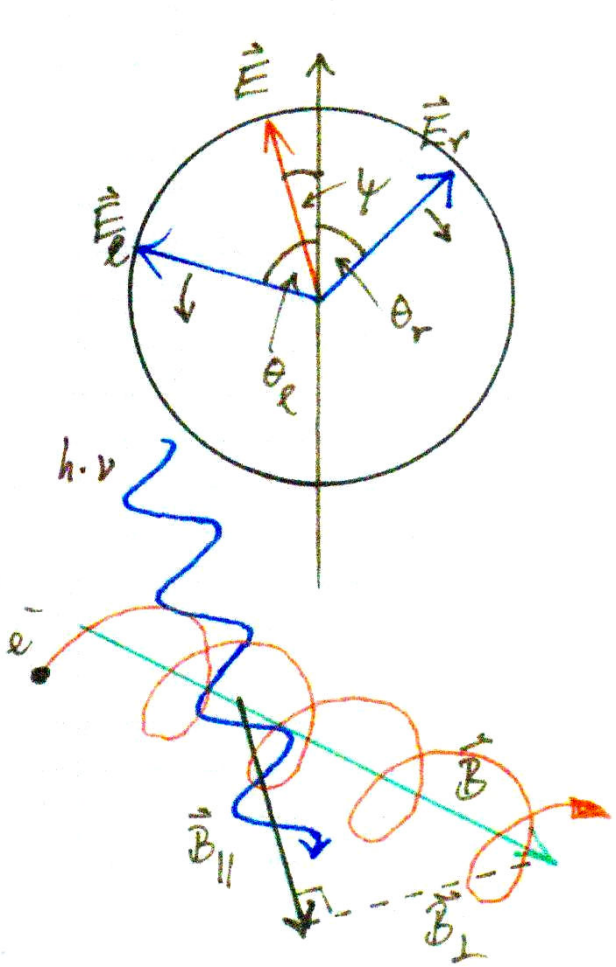

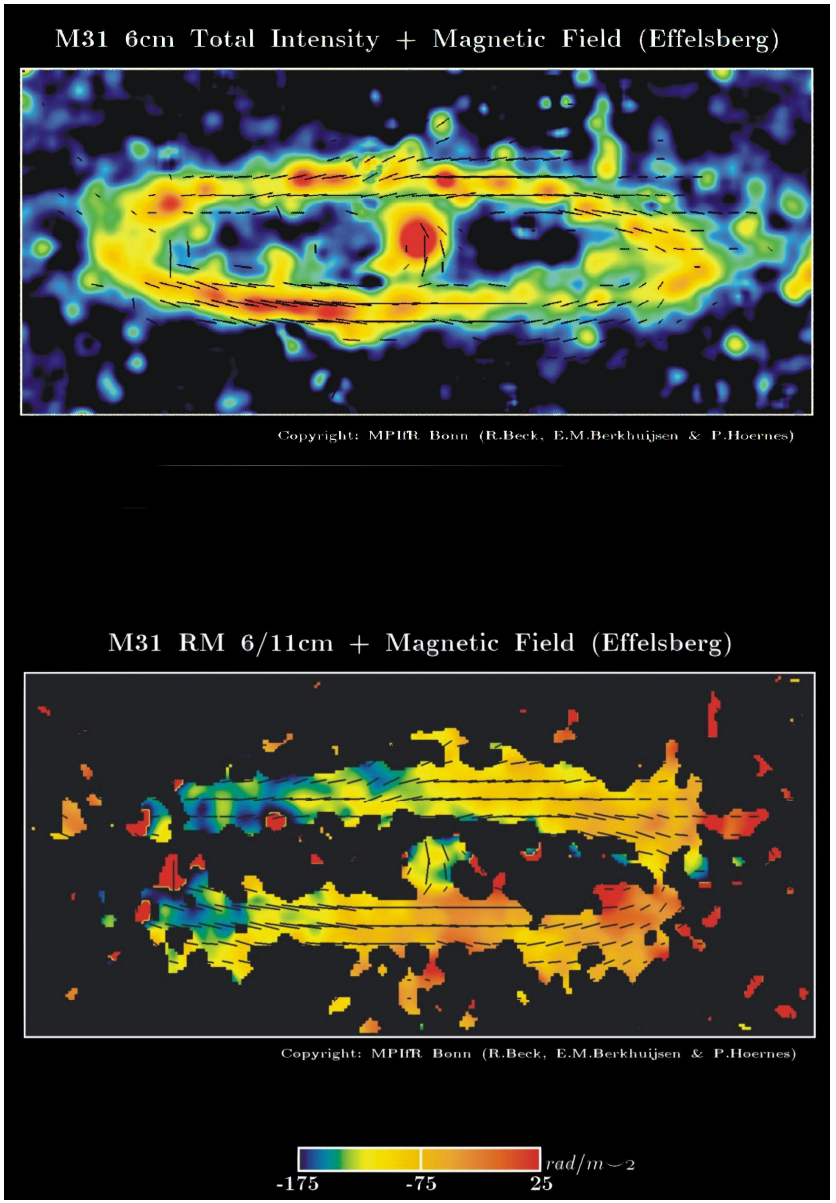

3.3.2 Depolarisation

Faraday depth, dispersion function Φ(r)

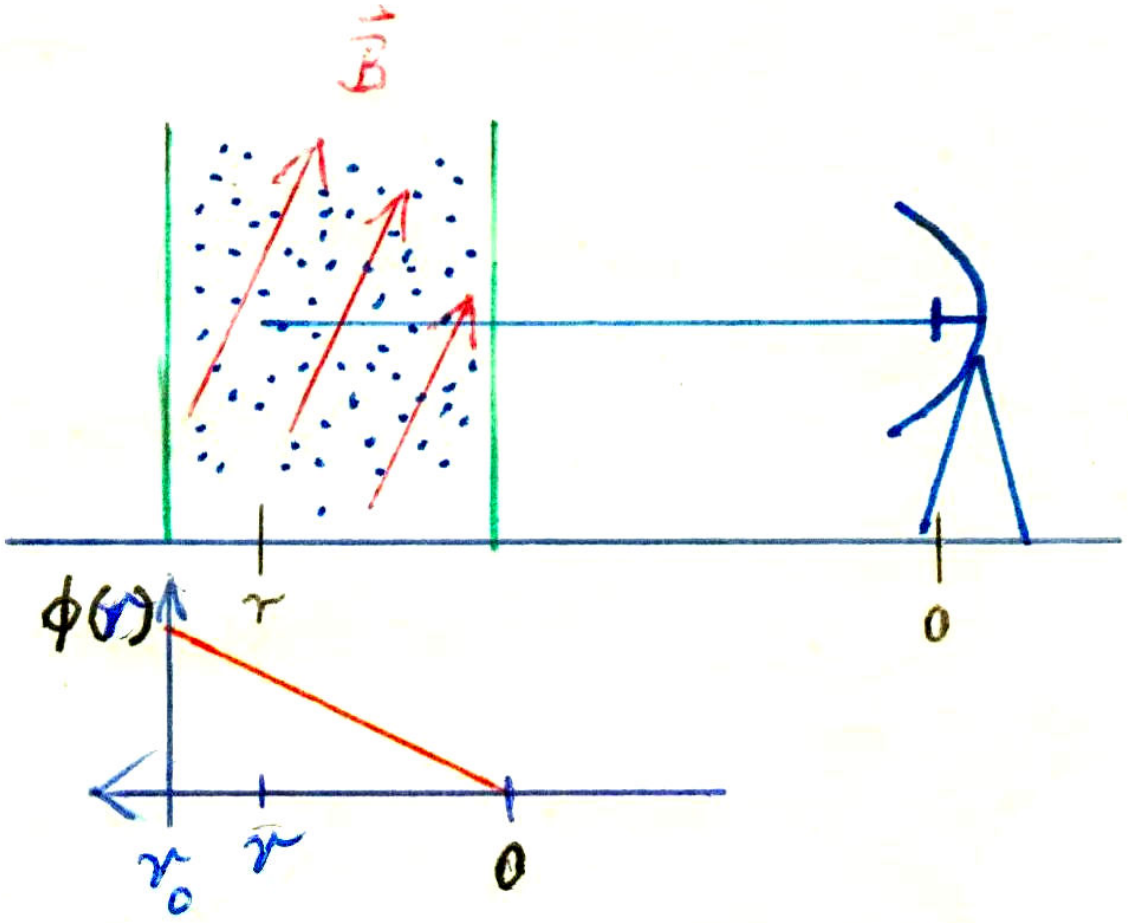

unresolved foreground screen

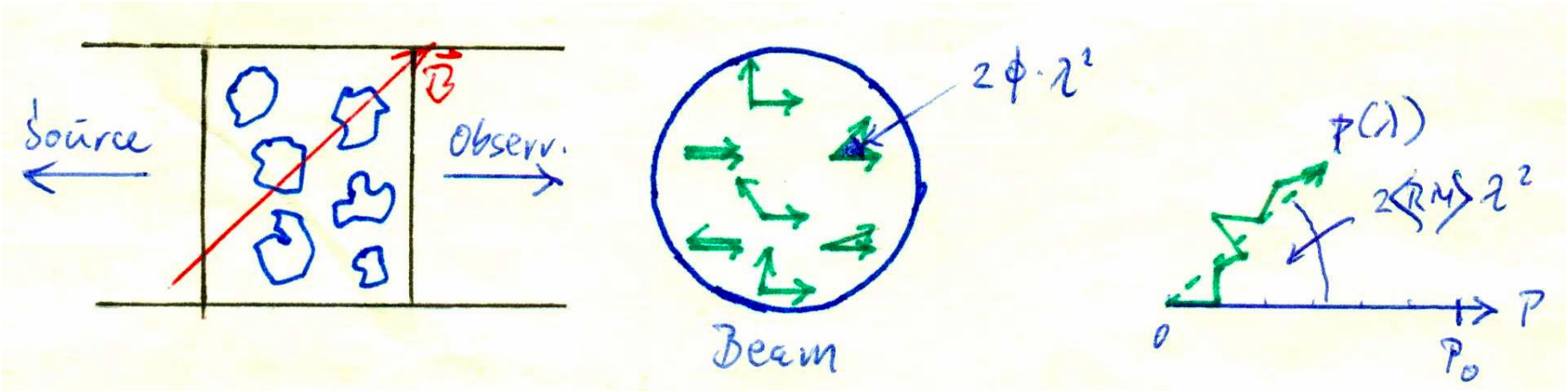

internal Faraday depolarisation

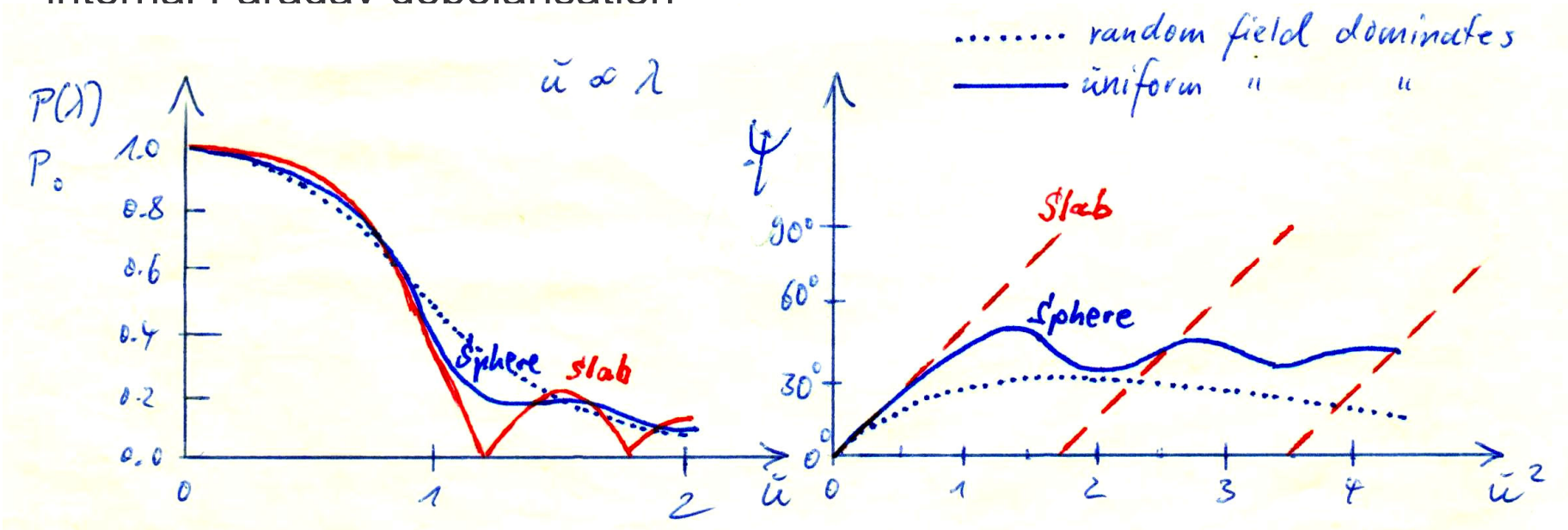

Degrees of linear polarisation

of 143 B3 radio sources observed

at 20, 11, 6, 2.8 cm wavelength …

… and resulting Faraday rotation

(Klein et al. 2003)

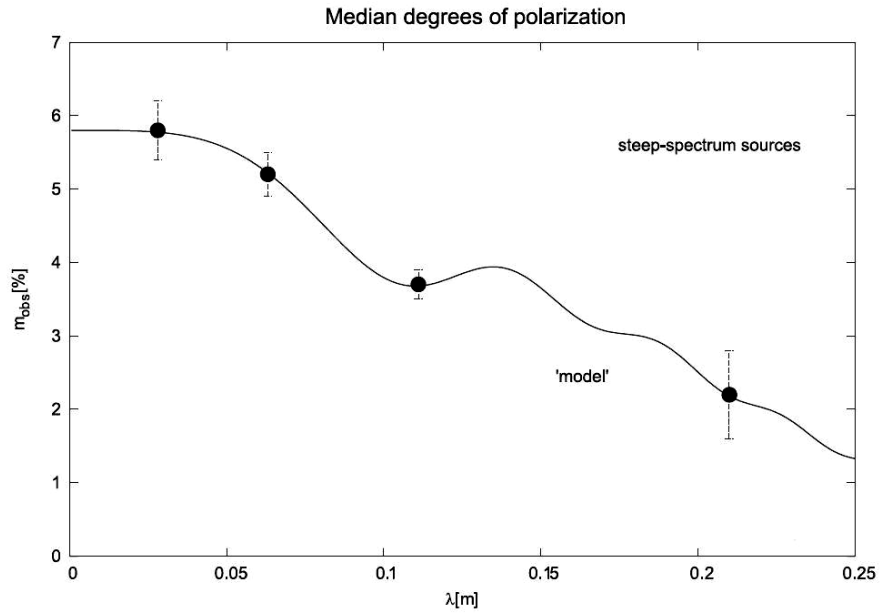

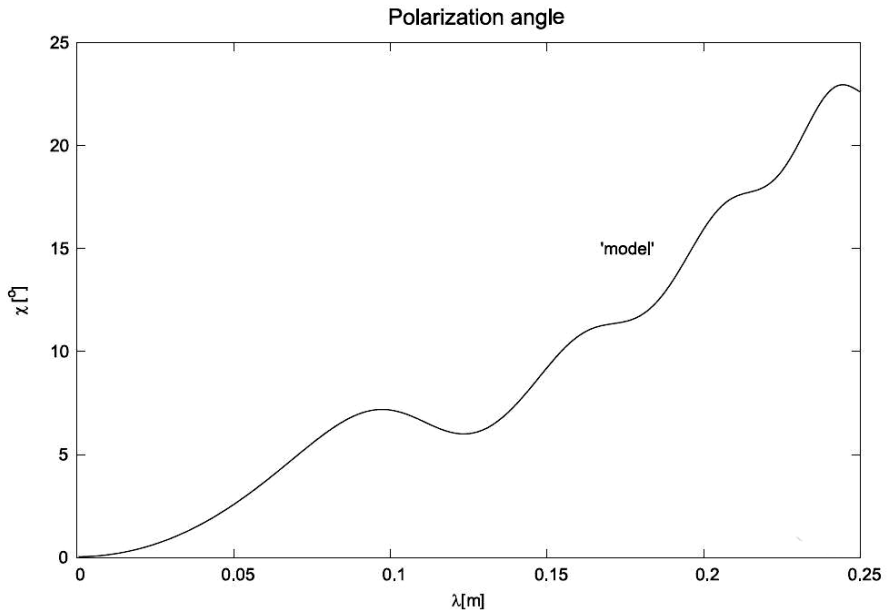

different distributions of

thermal and relativistic

electrons

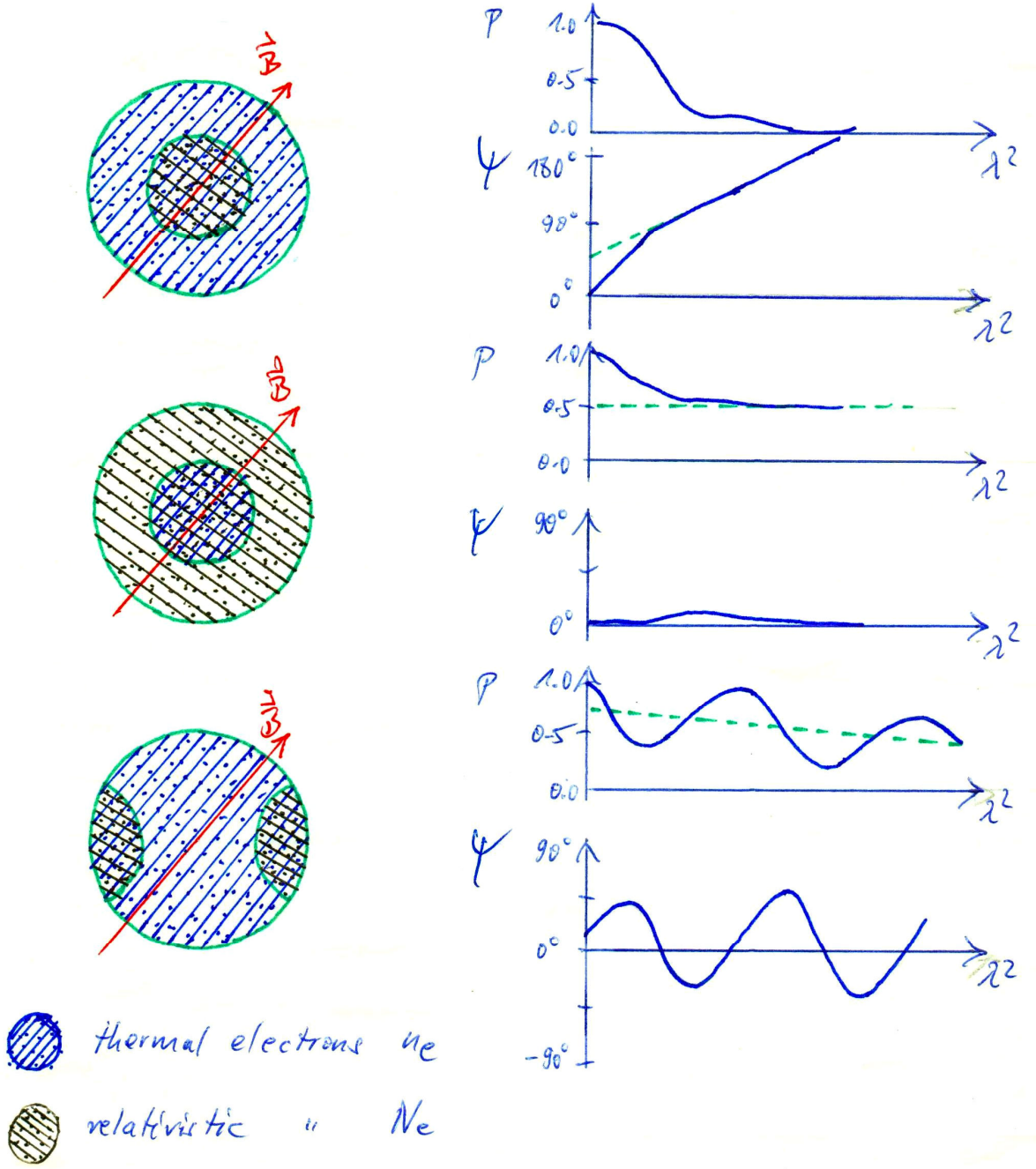

3.3.3 Rotation measure synthesis

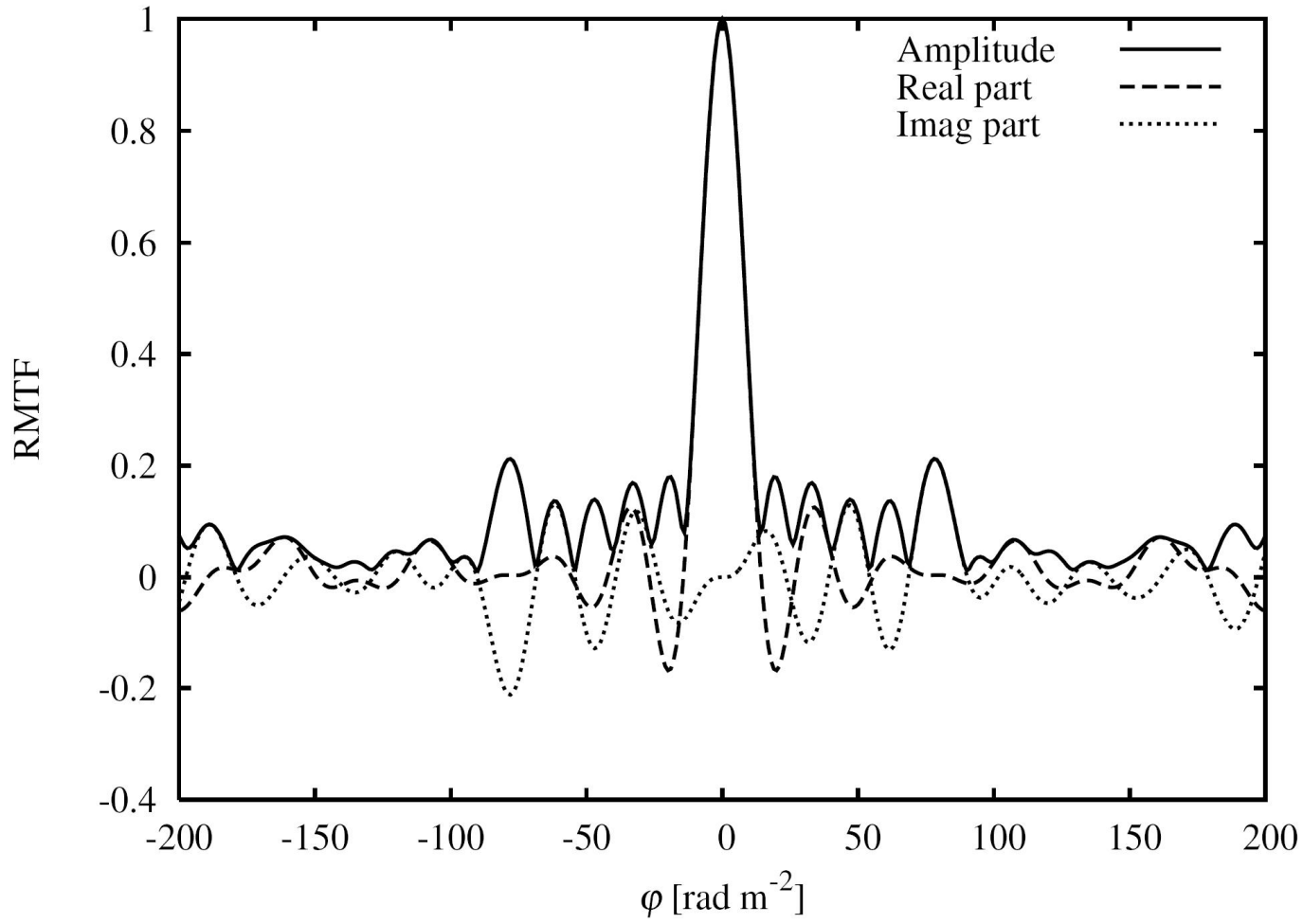

Rotation Measure Transfer Function of WSRT observations
(126 channels, 315 – 360 MHz, Brentjens & de Bruyn 2005)

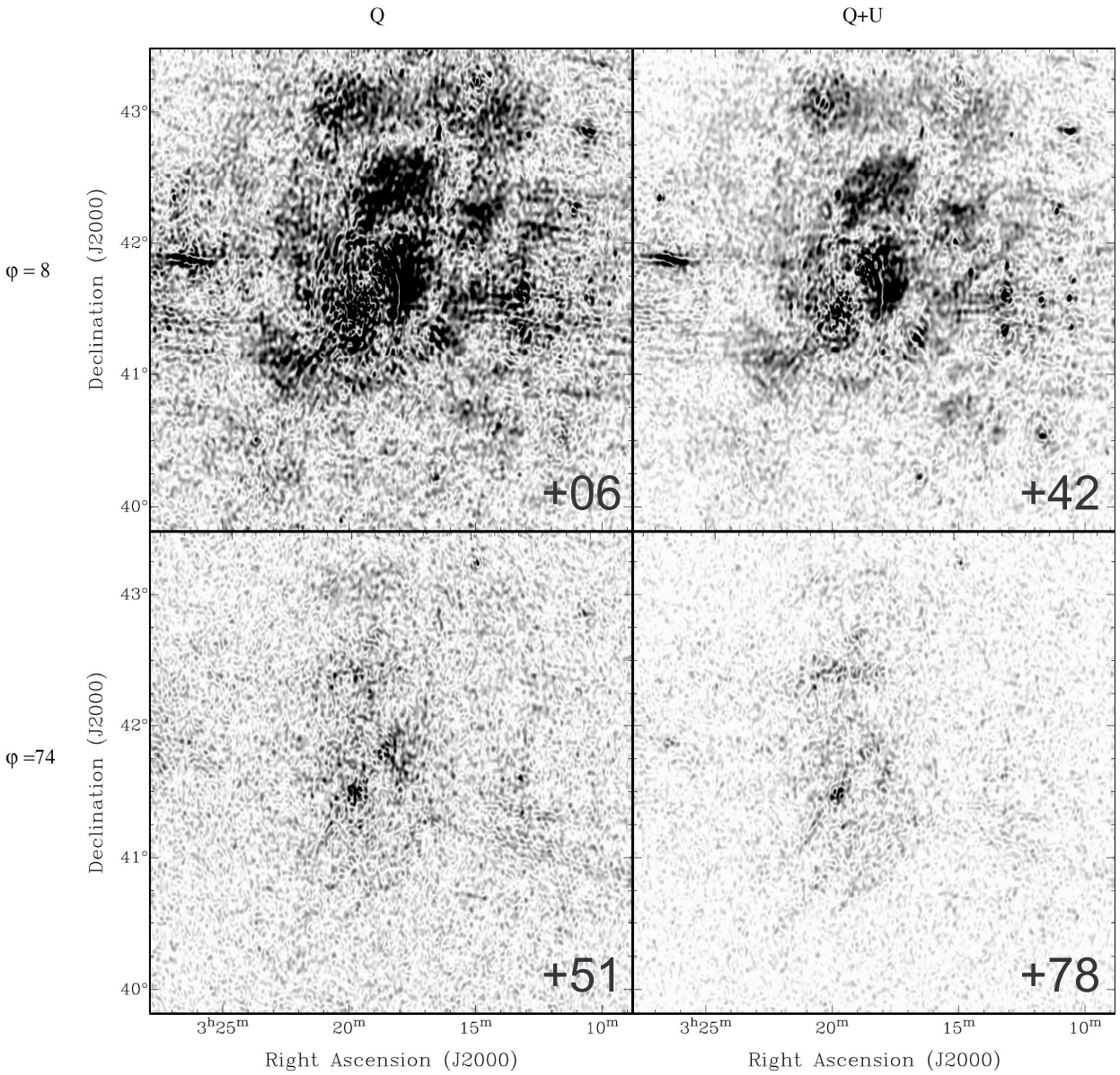

Examples of RM synthesis towards the Perseus Cluster at λ = 90 cm; frames are shown at +6, +42, +51, +78 rad m^{-2} (Brentjens & de Bruyn 2006)

synchrotron-emitting and Faraday-rotating slab, e.g.

Galactic foreground at -2 rad m^{-2} < Φ < +2 rad m^{-2}
plus
distant radio lobe at Φ = +10 rad m^{-2}

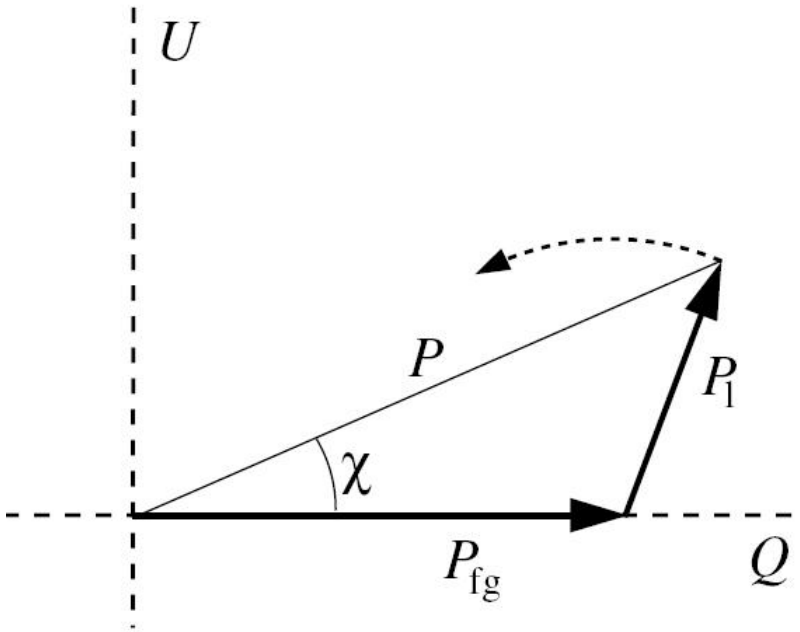

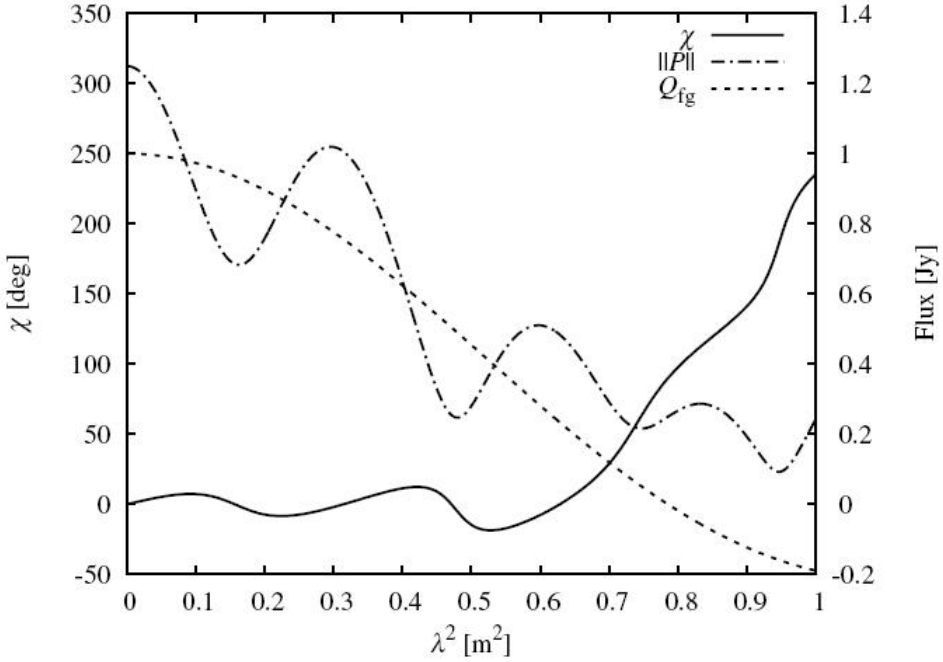

(from Brentjens & de Bruyn, 2005)

3.3.4 Zeeman effect

differential measurement

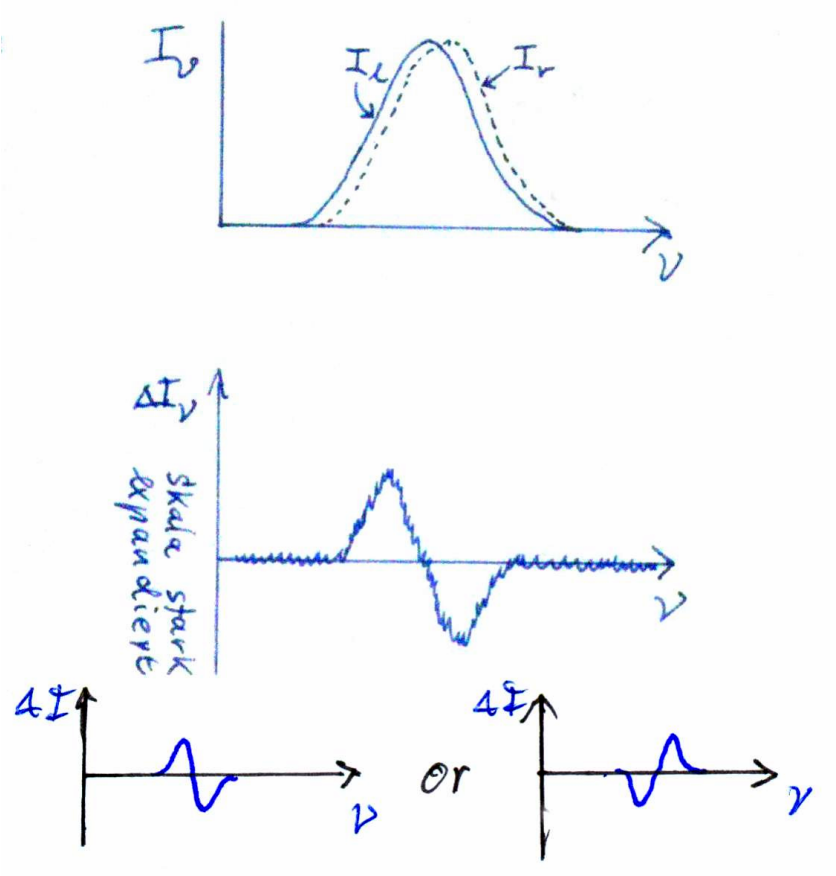

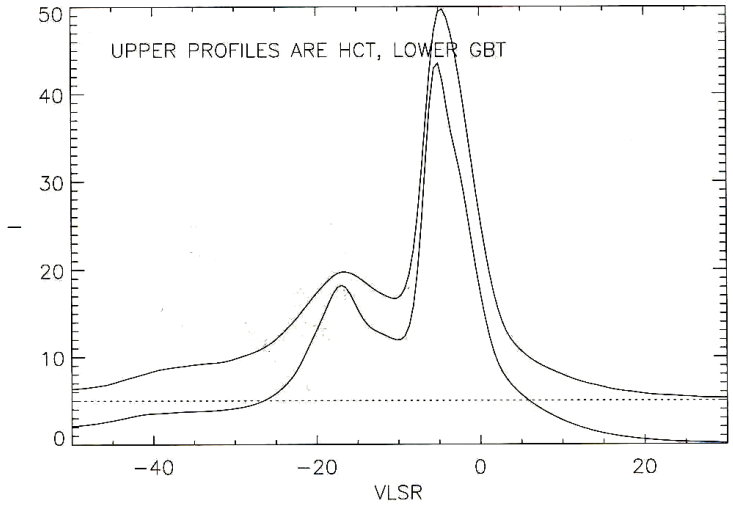

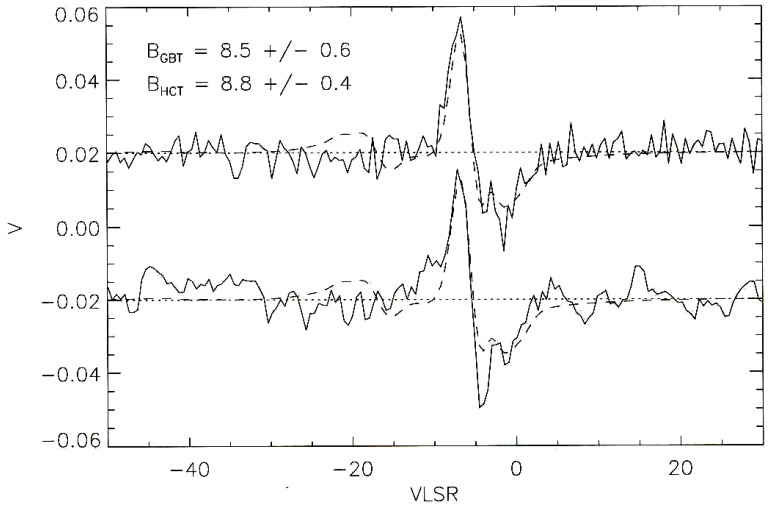

3.3.5 Polarised dust emission

B-field in NGC 1333 IRAS 4A from dust polarisation at 877 μm with the SMA